Journal of Power Sources, 26 (1989) 139 - 159

THE KINETICS OF POROUS INSERTION ELECTRODES

S. ATLUNG* and K. WEST
The Technical University of Denmark, DK 2800, Lyngby (Denmark)

Summary

The kinetics of porous electrodes with an insertion compound as active material is a compound function of the kinetics of the insertion material and transport of inserted ions in the electrolyte-filled pores. The insertion compound and the electrolyte transport are first treated separately and then combined in the treatment of the porous electrode. The overvoltage and the materials utilization for the insertion compound are treated in terms of simple, solid state diffusion and a potential/composition dependence based on an idealized model with first order interactions.

Transport in the electrolyte is treated using transport equations which take into consideration cross diffusion terms using the molar conductance. From this treatment an estimate of the conditions necessary to avoid depletion of electrolyte salt in the pores is derived.

The concepts of load factors for the insertion compound and for the electrolyte part of the electrode are introduced to express the severity of the discharge in relation to the transport rates in the systems.

The couplings between the insertion reaction and the transport in the pores are defined. Based on these the potentials and concentrations in the porous electrode during discharge can be found.

As an example, results from such calculations on a typical porous TiS_2 electrode with liquid electrolyte are presented. The influence of electrode thickness and porosity is demonstrated and a contour representation of the influence of the load factors on the materials utilization is shown.

It is demonstrated that a low mobility for the anion in the electrolyte is an advantage. In consequence, a theory for composite electrodes using solid electrolytes is developed. It is shown that this electrode behaves as a non-porous insertion electrode with a much enhanced transport rate.

Introduction

Most efforts to construct a rechargeable Li or Na-battery have been directed towards the use of insertion compounds as active material for the positive electrode.

*Author to whom correspondence should be addressed.

0378-7753/89/$3.50

When it comes to the design of practical batteries it is immediately obvious that in order to realize the high theoretical energy density of the alkali metal/insertion compound systems, the batteries must be constructed with porous electrodes.

The theory of porous electrodes has been intensively studied, but the work in this field has mostly been directed towards the problems associated with fuel cells and the lead–acid battery. The results from these studies are not easily adapted to the porous insertion electrode. The reason is that the behaviour of this electrode is controlled primarily by the following factors:

(i) The equilibrium electrode potential is usually very dependent on the degree of discharge.

(ii) The working potential is influenced by transport of the inserted ions in the solid electrode phase.

(iii) The mobility of ions in electrolytes compatible with the alkali metal negative electrode is much lower than the mobilities in aqueous electrolytes. Consequently, the influence of electrolyte transport is more pronounced than for aqueous systems.

Principles of porous electrodes

A porous electrode can be considered as consisting of two contiguous interwoven networks. The insertion compound network consists of particles in contact with each other. This network must be electronically conducting. The other network consists of the electrolyte-filled pores. They are in contact with the separator electrolyte positioned between the two electrodes. The ions participating in the insertion reaction and originating from the negative electrode migrate through the separator into the pores and through these to the site in the interior of the electrode where they react with the insertion compound. The characteristic feature of the porous electrode is, therefore, that the electrode reaction is distributed in space.

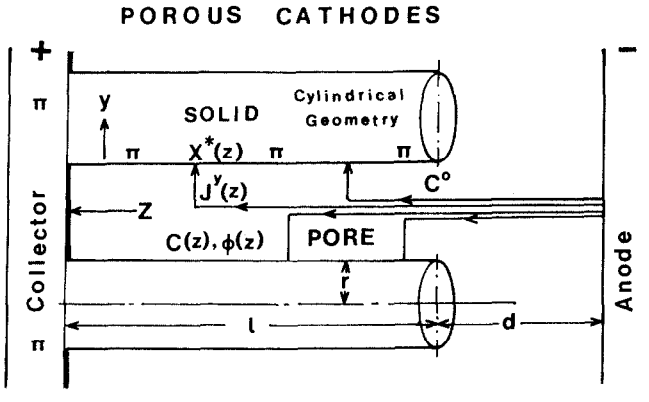

Fig. 1. Model of porous insertion electrode. Cylindrical geometry.

Figure 1 shows a very simplified model consisting of long cylinders of insertion compound in contact with the current collector. The pores between the cylinders are filled with electrolyte.

The discharge current enters the electrode pores as a flux of ions. Gradually, through the electrode reaction, this current decreases and becomes zero at the bottom of the pore. The local electrode reaction current i_t can be found from the decrease in the ionic current, i_l. Neglecting geometric factors the basic relation for the porous electrode is:

$$i_t = -\frac{di_l}{dz} \tag{1}$$

where z is the space coordinate in the porous system. The behaviour of the porous electrode is therefore equally influenced by the current and transport in the electrolyte network and by the discharge kinetics of the insertion compound.

Discharge of the insertion compound

The discharge of insertion electrodes can be formulated as:

$$\delta A^+ + \delta e^- + HA_x \longrightarrow HA_{x+\delta}$$

where A^+ is the inserted ion and HA_x is the partially inserted "host" compound. δ expresses a differential increase in the degree of insertion. In order to utilize the entire amount of insertion material the reacting ion must be transported away from the surface and distributed in the interior of the insertion compound particle. This transport takes place as solid state diffusion. The driving force is the gradient in chemical potential of the inserted ion caused by the abundance of this ion near to the surface.

Only a limited number of sites are available for the inserted ion. A convenient measure for the concentration is the relative local occupancy X, equivalent to the ratio of the local concentration c_s to the saturation concentration c_s^0. Considering that only $1 - X$ sites are available, the unidirectional flux density, j, can be found as [1]

$$j = -bX(1-X)\frac{d\mu_s}{dy} \tag{2}$$

where μ_s is the chemical potential of the inserted ion, y is the space coordinate, and b is a mobility.

The ionic transport is necessarily accompanied by rearrangement of the electron distribution. However, in most insertion compounds the electronic mobility is much larger than the ionic mobility, and therefore $d\mu_s$ will control the transport. There are no general rules for the relation between μ_s and X, but for analyzing the characteristic behaviour of insertion electrodes, we may use an ideal model substance. If we consider all available sites to be equivalent, statistical mechanics gives [2]

$$\mu_s = \mu^{\ominus} + RT \ln \frac{X}{1-X} \tag{3}$$

which combined with eqn. (2) gives

$$j = -RTb \frac{dX}{dy} \tag{4}$$

which is equivalent to Fick's first law with a diffusion coefficient $D_s = RTb/c_s^o$. A much better approximation is obtained if we allow for first order interactions between the inserted ions. If these are weak we get [1]

$$\mu_s = \mu^{\ominus} + RT \left(\ln \frac{X}{1-X} + fX \right) \tag{5}$$

where the interaction energy is contained in the factor f, which is positive for repulsive interactions. Combining eqns. (2) and (5) gives

$$j = -RTb(1 + fX(1-X)) \frac{dX}{dy} \tag{6}$$

which describes diffusion with a concentration dependent diffusion coefficient.

Unfortunately the use of a concentration dependent diffusion coefficient prevents analytical solutions of the transport problem, and impedes a simple evaluation of the influence of the transport on the discharge behaviour. For this reason the following discussion will be conducted using the simple form, eqn. (4). The solid state diffusion coefficient, D_s, should be considered as an average value. In numerical work, however, the use of eqn. (6) presents no problems and is recommended. In any case, transport by diffusion implies that the value of X at the surface, X^*, is higher than the average value, which is equal to the degree of discharge. This is illustrated in Fig. 2, which depicts the development of the concentration profile for two different particle shapes during discharge. When X^* becomes equal to unity, further insertion is impossible and the discharge ends. At this point the average value of X and, consequently, the utilization of the insertion material, will be less than one. The amount of material not utilized can be found from the shape of the X profile through the particle.

To find an analytical expression for this profile we must solve the general mass conservation relation $\partial c/\partial t = -\partial j/\partial y$. The concentration gradient at the surface is

$$\left.\frac{dX}{dy}\right|_{\text{surface}} = \frac{-i_y}{Fc_s^o D_s} \tag{7}$$

where i_y is the discharge current density. The mass conservation relation gives, with j inserted from eqn. (4)

$$\frac{\partial X}{\partial t} = D_s \frac{\partial^2 X}{\partial y^2} \tag{8}$$

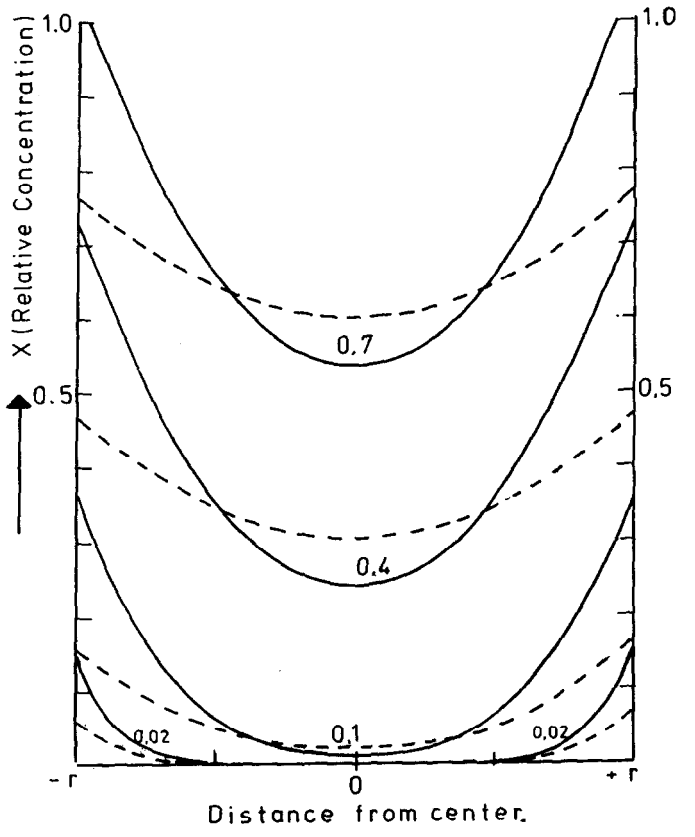

Fig. 2. Concentration profiles in particles for different times, indicated as t/τ_D. ——, plane geometry; — — —, spherical geometry; load factor, $L_s = 1$.

The boundary condition on the insertion compound/electrolyte interface is given by the discharge mode. If we assume a constant current discharge, eqn. (7) with constant i_y is the proper condition to use.

The other boundary condition is chosen at the center or symmetry plane of the particle where $dX/dy = 0$. In this way we introduce the particle size, defined as the distance, r, from the surface to the symmetry point or plane. The magnitude of the particle size has two aspects. First, because, for batteries, the discharge current will be specified, not as the interfacial current density, but as a current, I, *e.g.*, per unit volume electrode. The interfacial area per unit volume is determined by r and the geometry of the particle. The ratio between area and volume is s/r, where s is 1, 2, or 3 for plane, cylindrical, and spherical particles, respectively. Thus for given I the current density decreases for decreasing r.

The other effect of the particle size is that the time for transport through the entire particle depends on r. The time constant for diffusion is:

$$\tau_s = \frac{r^2}{D_s} \tag{9}$$

τ_s must be small compared with the required discharge time in order to obtain a uniform utilization.

With the boundary conditions discussed, the solution of eqn. (8) is straightforward and gives an expression for X as a function of the time and position [3].

As illustrated in Fig. 2, for small times the insertion reaction has not penetrated to the center of the particle. The diffusion is "semiinfinite" and X varies with time according to a $t^{1/2}$-law (*cf.* the "Sand" equation). The utilization of the material is low, less than 50%, and for this reason this part of the discharge is, as a rule, uninteresting from a battery point of view. For larger times the semiinfinite diffusion transforms into diffusion in the domain bounded by the particle size. The degree of insertion at the center of the particle increases and the profile becomes parabolic. This profile is then displaced linearly with time against higher values of X.

The general solution for the dependence of the surface value X^* on time can be found as [2, 3]:

$$X^* = \frac{Ir^2}{Fc_s^o D_s s}\left(s\frac{D_s t}{r^2} + \frac{1}{s+2} - 2\text{"}\Sigma\text{"}\right) \tag{10}$$

The term "Σ" signifies an infinite sum of exponentials of the form: $[\exp(-\alpha_i^2 t/\tau_s)]/\alpha_i^2$, where α_i, for example, for plane particles is $i\pi$, $i = 1 \ldots \infty$. For $t > \tau_s/3$ the "Σ" term can be neglected. The charge per unit volume which the electrode can deliver if all particles are uniformly saturated, Q_o, is Fc_s^o. Equation (10) without "Σ" can then be written as:

$$X^* = \frac{It}{Q_o} + \frac{Ir^2}{Q_o D_s}\frac{1}{s(s+2)} \tag{11}$$

As It is the charge delivered at time t, the first term is the overall degree of discharge, U. Q_o/I is termed the stoichiometric discharge time, τ_D, *i.e.*, the discharge time with the given current I if the electrode could be utilized 100%. τ_D resembles the measure used in the battery industry to characterize the discharge rate, *e.g.*, a 3 h discharge.

$Ir^2/Q_o D_s$ is the ratio between the two characteristic times: τ_s/τ_D. This ratio is termed the "load factor", L_s. Because τ_s is a measure for diffusion resistance and τ_D for the reaction rate required, L_s is a measure of the severity of the discharge. With these battery oriented parameters eqn. (11) can be written:

$$X^* = U + \frac{L_s}{s(s+2)} \tag{12}$$

The maximum utilization, U_{max}, is obtained when $X^* = 1$:

$$U_{max} = 1 - \frac{L_s}{s(s+2)} \tag{13}$$

The values of the load factor where eqns. (12) and (13) are valid is limited by the assumption $t > \tau_s/3$ at the saturation point. This gives an upper limit for L_s which is 1.5, 2.2, and 2.5 for plane, cylindrical, and spherical particles, respectively.

In the considerations above it was assumed that surface saturation is the dominating cause of the end of discharge. This requires that enough A^+ ions are available in the electrolyte at the interface. Also, to apply eqns. (10) - (13) on a porous electrode, the current distribution must be uniform. These two conditions are only fulfilled in a favourably limiting case.

The working potential

The preceding section was only concerned with the coulombic capacity. The working potential as a function of the degree of discharge is, however, necessary to explain the operation of porous electrodes. Also, the working potential together with the coulombic capacity determines the energy output.

From thermodynamic considerations the following expression for the equilibrium potential can be derived [4]:

$$(\pi - \phi) = \frac{1}{F}(\mu_+ - (\mu_s + \mu_s^e)) \tag{14}$$

π is the Fermi potential in the insertion compound, ϕ the Galvani potential in the electrolyte, μ_+ the chemical potential of A^+ in the electrolyte and μ_s^e the chemical potential of electrons in the insertion compound. The electronic term may play a role for some compounds, but for our model compound we shall assume that this term is constant because the intrinsic electron concentration is high. For μ_s we shall use eqn. (5) and for the electrolyte term the ideal solution value: $RT \ln c_1$, where c_1 is the concentration of A^+ in the electrolyte. For the working potential, E, we must use the interfacial concentrations indicated by superscript * and add a transfer overvoltage term, η, depending on the interfacial current density.

Then the working potential of the model substance is:

$$E = E^\circ + \frac{RT}{F}\left(\ln c_1^* - \ln \frac{X^*}{1 - X^*} - fX^*\right) + \eta \tag{15}$$

where E_o is a standard potential.

To estimate the significance of the terms in eqn. (15) TiS_2 can be used as an example [5]. In Fig. 3, measured values of E for TiS_2 are depicted together with the curve calculated from eqn. (15) with $f = 20.5$. Note that in the range $0.05 < X < 0.95$ the potential decrease is 550 mV, but only 150 mV originates from the $\ln X/(1 - X)$ term.

The influence of the charge transfer term, η, can be estimated from measurements by a.c. small signal impedance spectroscopy on TiS_2 single

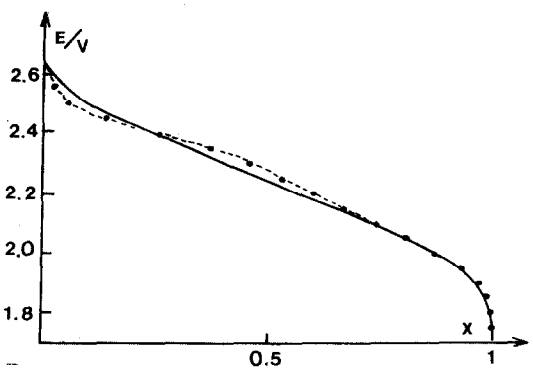

Fig. 3. Dependence of e.m.f. on X for TiS_2. - - - -, Measured points; ——, calculated from eqn. (15), with c_l included in E^o and $f = 20.5$.

crystals [6]. The charge transfer resistance was estimated to be 20 - 150 ohm cm^2 at $X = 0.5$. As the current density at the surface of a 10 μm spherical TiS_2 particle discharged at the 3 h rate is *ca.* 0.05 mA cm^2, the transfer overvoltage is estimated to be 1 - 10 mV, which is quite insignificant compared with the overall voltage change during discharge. This is considered typical for insertion electrodes, as the charge transfer does not include formation of new phases or electron transfer. In the following the charge transfer term in eqn. (15) is neglected.

To calculate the working potential as a function of discharge time, X^* is found from the solution of eqn. (8), and this value is used in eqn. (15). During most of the discharge the X^* terms dominate, but in porous electrodes c_l^* may approach zero in the interior of the electrode and cause a high overvoltage.

Transport in the electrolyte

The electrolytes used may be liquid, polymeric, or solid. Solid electrolytes should be fast ion conductors. Electrode systems using these electrolytes will be treated separately in a later section.

The following concerns liquid and polymeric electrolytes. The electrolyte salt used in these is supposed to be a 1:1 salt of A^+. The ion fluxes are determined by the gradients in the electrolyte concentration and in the Galvani potential. These gradients depend on the magnitude of the discharge current. As a rule they vary with the position in the pore, and with time.

To model the ionic transport in the first approximation the Nernst–Planck equation can be used. Using the ionic current to express the electrical transport we get:

$$j_+ = -D_l \frac{dc_l}{dz} + n_+ \frac{i_l}{F} \tag{16a}$$

$$j_- = -D_1 \frac{dc_1}{dz} - n_- \frac{i_1}{F} \tag{16b}$$

where j are the flux densities and n the transport numbers, + and − signifies cation and anion, respectively. The ionic diffusion coefficients D_+ and D_- are combined in the salt diffusion coefficient D_1

$$D_1 = \frac{2D_+D_-}{D_+ + D_-}$$

$$n_+ = \frac{D_+}{D_+ + D_-}; \qquad n_- = \frac{D_-}{D_+ + D_-} \tag{17}$$

The use of the Nernst–Planck equation is limited to situations where one can neglect the influence of the movement of one ion on the other. This effect plays an important role for transport in an electric field, which is clearly indicated by the marked dependence of the molar conductance on concentration.

To take account of this, transport equations derived from the Stephan–Maxwell equations can be used [7]. These equations connect the driving forces on the ions with three friction coefficients, $K_{+,o}$, $K_{-,o}$ and $K_{+,-}$, and the velocities v_+, v_- and v_o, where "o" signifies the solvent. The forces, in their turn, are given by the negative gradients in the electrochemical potential $\bar{\mu}$:

$$-\frac{d\bar{\mu}_+}{dz} = K_{+,o}(v_+ - v_o) + K_{+,-}(v_+ - v_-)$$

$$-\frac{d\bar{\mu}_-}{dz} = K_{-,o}(v_- - v_o) + K_{+,-}(v_- - v_+) \tag{18}$$

To arrive at simple expressions, some simplifications are used. First, the solvent is used as reference frame for the fluxes and currents. This gives $v_+ - v_o = j_+/c_1$, $v_- - v_o = j_-/c_1$ and $v_+ - v_- = i_1/Fc_1$.

Second, we assume that the concentration of the solvent is constant, independent of c_1. Then $K_{+,o}$ and $K_{-,o}$ are concentration independent and can be connected with the Nernst–Planck diffusion coefficients through $K_{i,o} = RT/D_i$. However, the cross coefficient $K_{+,-}$ is very concentration dependent, approaching zero at infinite dilution.

Finally, we shall use concentrations in the expression for $d\bar{\mu} = RTd\ln c + zFd\phi$, neglecting the gradient in activity coefficients. After some eliminations and rearrangements we get:

$$j_+ = -\frac{2D_+D_-}{D_+ + D_-}\frac{dc_1}{dz} + \frac{D_+}{D_+ + D_-}\frac{i_1}{F}$$

which is equivalent to eqn. (16). Thus, this form includes the interaction between cation and anion transport.

When current is used as an independent variable, a relation for the potential as a function of c_1 and i_1 is needed. We get:

$$\frac{d\phi}{dz} = -\frac{RT}{F}(n_+ - n_-)\frac{d\ln c_1}{dz} - \frac{i_1}{c_1\Lambda} \tag{19}$$

where Λ is the molar conductance at the concentration c_1.

Time dependence of the electrolyte concentration

The development of the concentration in the pores during discharge can be found from the mass conservation relation. The simple form $\partial c/\partial t = -\partial j/\partial z$ can be used if the diffusing substance does not participate in the electrode reaction. This is the case for the anion. Thus by using j_- from eqn. (16b) we get the following relation for the change of c_1 with time t and position z:

$$\frac{\partial c_1}{\partial t} = D_1\frac{\partial^2 c_1}{\partial z^2} + \frac{n_-}{F}\frac{\partial i_1}{\partial z} \tag{20}$$

$-\partial i_1/\partial z$ is equal to the local discharge current, eqn. (1). In the general case this term cannot be found explicitly as a function of t and z.

As a limiting case, the most favourable discharge condition is a uniform reaction distribution through the entire electrode. di_1/dz is then constant and eqn. (20) can be solved. For this purpose we shall not use the discrete geometrical model shown in Fig. 1, but a modification of the "macro-homogeneous" one-dimensional model proposed by Newman and Tobias [8]. In this model the electrode is treated as a continuum with concentrations, c', and transfer current, i_t, calculated on the basis of unit electrode volume. Current and flux densities are measured per unit electrode cross-sectional-area. The electrode structure is defined by an overall porosity, p, and a tortuosity factor, θ. The concentrations are $c_1' = pc_1$ and the effective diffusion coefficient, $D_1' = D_1/\theta^2$ [9]. The z axis does not follow the tortuous path of the pores, but is perpendicular to the electrode surface. The origin is placed at this surface and discharge current is counted positive. The current collector is then positioned at $z = l$, where l is the electrode thickness.

If the discharge current density of the electrode surface is i°, eqn. (20) gives, for a uniform reaction distribution:

$$\frac{\partial c'}{\partial t} = D_1'\frac{\partial^2 c'}{\partial z^2} - n_-\frac{i^\circ}{Fl} \tag{21}$$

If we assume that the concentration outside the electrode surface is constant, c_1°, the boundary conditions are:

$$\begin{aligned} z &= 0 \qquad c' = pc_1^\circ \\ z &= l \qquad dc'/dz = 0 \end{aligned} \tag{22}$$

The solution can be derived from the corresponding heat conduction problem [10]. This solution contains, as with eqn. (10), an infinite sum of negative exponentials of the form:

$$[\exp-((n + 1/2)\pi)^2 t/\tau_1]/[(n + 1/2)\pi]^3 \qquad n = 0, \ldots, \infty$$

τ_1 is the time constant for electrolyte diffusion in the electrode:

$$\tau_1 = \frac{l^2}{D_1'} \tag{23}$$

For $t > \tau_1$ the exponentials vanish and the solution degenerates to the stationary profile found for $\partial c/\partial t = 0$. This approximation is valid in most cases: *e.g.*, for a 0.5 mm electrode with $D_1' = 10^{-6}$ cm^2 s^{-1} τ_1 is 0.7 h, *i.e.*, considerably shorter than is required by most discharge schemes. The stationary solution is:

$$c' = c_1^0 p + \frac{n_- i^0}{FD_1'}\left(\frac{z^2}{2l} - z\right) \tag{24}$$

To utilize the entire electrode, electrolyte depletion must be avoided. Consequently, we must require $c' > 0$ for $z = l$. This gives an upper limit for l:

$$l < \frac{2FD_1 c_1^0 p}{n_- i^0 \theta^2} \tag{25}$$

For a given discharge rate specified as τ_D, i^0 depends on the amount of insertion compound, *i.e.*, on l and $1 - p$, and D_1/n_- is $2D_+$. This gives:

$$l^2 < \frac{4D_+ c_1^0 p}{\theta^2 c_s^0 (1-p)} \tau_D \tag{26}$$

Equation (26) provides the possibility of evaluating the interplay between the design parameters: l, p and c_1^0, and the discharge rate. Note, in particular, the large influence of the electrode thickness on the maximum allowable discharge rate.

For the insertion compound the load factor τ_s/τ_D was instructive to use. We may also consider a load factor, L_1, for the electrolyte network, defined as τ_1/τ_D. To avoid electrolyte depletion we require

$$L_1 < \frac{2c_1^0 p}{n_- c_s^0 (1-p)} \tag{27}$$

The fraction $c_1^0 p/(c_s^0(1-p))$ is the ratio between the charges in the two networks. As c_s^0 is much larger (*e.g.*, 25 mol dm^{-3}) than c_1^0, the limit for L_1 is small, of the order of 0.1 - 0.2. This sets rather strict limits on the electrode thickness or the discharge rate.

A uniform reaction distribution, as assumed in the discussion above, is never obtained in a porous insertion electrode. However, it is likely that the relations (25) - (27) give good practical guidelines for the design of electrodes,

which are not limited by electrolyte depletion. This may be important where porous electrodes are used for evaluating new insertion materials.

Modelling of the porous electrode

In the preceding sections the insertion compound and the electrolyte networks which together constitute the porous electrode, were discussed separately. Limiting cases where one of these networks limits the electrode performance, and where simple mathematical expressions are available, were investigated. Probably none of these cases is optimal for the design of an electrode for a real battery.

The transport in the electrolyte is coupled to the transfer process and the transport in the insertion compound in two ways. One of these was expressed in eqn. (1), which states that the local discharge current is given by the gradient of the current in the electrolyte. The other coupling originates from the dependence of the potential in the electrolyte, ϕ, on the local electrode potential, $E = \pi - \phi$. π is the Fermi potential in the insertion compound. If the electronic conductivity is high, π has a constant value everywhere in the electrode. However, E varies with position in the electrode due to different degrees of insertion. This variation is for constant π transferred to the electrolyte potential:

$$d\phi(z, t) = -dE(z, t) \tag{28}$$

In this way E will influence the current and fluxes in the electrolyte. For a battery, the discharge potential E^* is measured between the positive current collector and the negative electrode. In the present context we shall measure the discharge potential between the current collector and a reference electrode placed close to the outer surface of the electrode ($z = 0$). This potential can be found as:

$$E^* = \pi_l - \pi_{Ref} = (\pi - \phi)_o - (\pi - \phi)_{Ref} - (\pi_o - \pi_l) \tag{29}$$

where the subscripts signify the z-coordinate.

For a high electronic conductivity $\pi_o - \pi_l$ can be neglected, and the electrode potential is consequently given by X^* and c_l^0 at the outer surface. If necessary the term $\pi_o - \pi_l$ can be found by integrating $(i^o - i_l)/\kappa_e$.

In order to calculate the discharge behaviour it is necessary to find X, c_l, ϕ and i_l as functions of time and position. This can be done by numerical solution of the set of coupled differential equations describing the transports in the porous electrode system. Transport in the insertion material is governed by eqn. (8) with the boundary condition, eqn. (7). i_y is found using eqn. (1), which for the porous system gives:

$$i_y = -\frac{r}{s(1-p)} \frac{di_l}{dz} \tag{30}$$

as the volume of insertion compound per unit electrode volume is $1 - p$ and the area to volume ratio is s/r.

Transport in the electrolyte pores is described by eqn. (20) and the local ϕ potential by eqn. (19). The coupling between the electrolyte and the insertion compound is then effected by combining an E/X relation, such as eqn. (15) with eqn. (28).

The boundary conditions for the whole system are given by the discharge mode and the concentration at the surface of the electrode. A convenient way to solve the system is a finite difference scheme as described by Brumleve and Buck [11].

Simulation of a TiS_2 porous electrode

Similar methods to those discussed above were used for simulating the discharge behaviour of a typical porous Li insertion electrode [12]. The TiS_2 electrode with an $LiClO_4$/PC electrolyte was used as an approximation to an ideal model electrode. The discharge mode investigated was constant current and the surface concentration of $LiClO_4$ was assumed constant. Other data used are listed in Table 1. The geometry factor 2 was chosen because for TiS_2 there is no Li-transport in the direction of the c-axis.

The simulated discharge curve and, for comparison, the equilibrium e.m.f., are shown in Fig. 4. We note the depression of the working potential and, at the end of discharge, a coulombic materials utilization of 80%.

The behaviour of the electrode during discharge is analyzed in detail in Fig. 5, where the distributions of c_l/c_l^o, X^* and i_y (in dimensionless units) are depicted for the times indicated in Fig. 4 (10, 50 and 80% utilization).

The controlling factor in this case is quite obviously the electrolyte salt distribution. At 50% utilization, the inner 20% of the electrode is already depleted of electrolyte, whereas the degree of discharge and the reaction

TABLE 1

Design data	
Electrode thickness (l)	0.5 mm
Particle radius (r)	0.5 μm
Porosity (p)	0.35
Tortuosity (θ) (assumed)	1
Stoichiometric discharge time (τ_D)	4.2 h
Current density (i^o)	5 mA cm^{-2}
Initial electrolyte concentration (c_l^o)	1 mol dm^{-3}
Materials data	
Saturation concentration of insertion compounds (c_s^o)	25 mol dm^{-3}
Solid state diffusion coefficient (D_s)	10^{-10} cm^2 s^{-1}
Geometry factor (cylindrical)	2
Salt diffusion coefficient (D_l)	2.6×10^{-6} cm^2 s^{-1}
Cation diffusion coefficient (D_+)	1.6×10^{-6} cm^2 s^{-1}
Anion transport number (n_-)	0.8

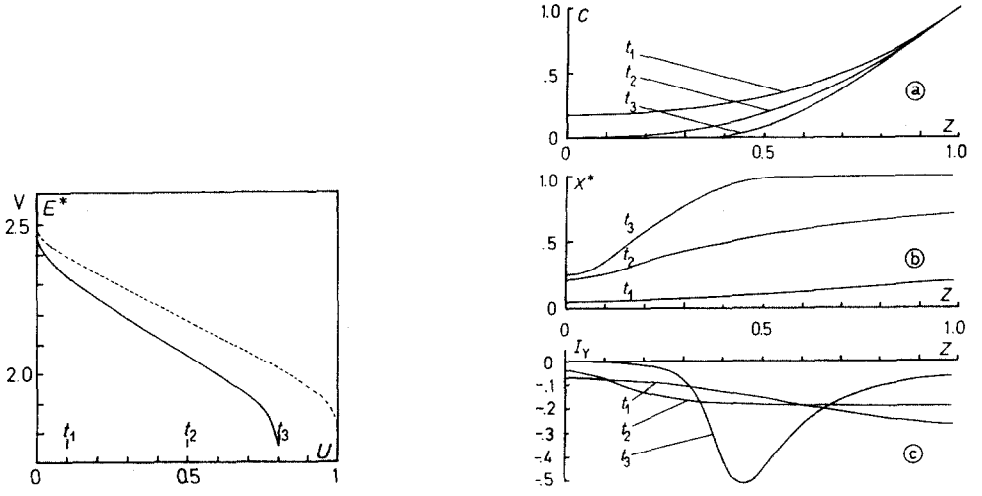

Fig. 4. Simulated constant current discharge curve for a TiS_2 porous electrode with data given in Table 1. For comparison e.m.f. equilibrium curve.

Fig. 5. Distribution of electrolyte concentration c, surface value of X and transfer current I_y (with sign reversed) in dimensionless units. The three sets of curves correspond to the discharge times (degree of discharge 10, 50 and 80%) indicated in Fig. 4.

current are reasonably well distributed. As the electrolyte depletion extends further, the outer parts of the electrode become completely discharged. The region where discharge can take place is thus squeezed between the electrolyte-depleted and the exhausted parts, resulting in the pronounced peak in the reaction current distribution.

The load factor for the electrolyte network is 0.064, whereas the limit according to eqn. (27) is 0.054. Thus, this simple consideration warns that electrolyte depletion might occur.

It is instructive to investigate how the electrode thickness and the porosity influence the discharge. Simulations were performed for a number of electrode thicknesses and porosities using a higher current (τ_D = 2 h) [13]. The results are shown in Fig. 6.

The large influence of these design parameters is remarkable and must be considered when designing practical batteries. The results reported above are typical for electrodes where the electrolyte transport is limiting. However, if the particle size is large, or the diffusion coefficient in the insertion compound very small, the transport in the solid phase may become limiting.

To rationalize the relations between the utilization and the discharge rate one can use the two load factors L_s and L_l. To make the results as general as possible it is an advantage to include the electrolyte concentration and the porosity in L_l. The new load factor L_l^* defined as the ratio between the time constant and the "discharge time" for the electrolyte: $lpc_l^\circ F/i^\circ$:

$$L_l^* = \frac{\tau_l}{\tau_D} \frac{(1-p)c_s^\circ}{pc_l^\circ} \tag{31}$$

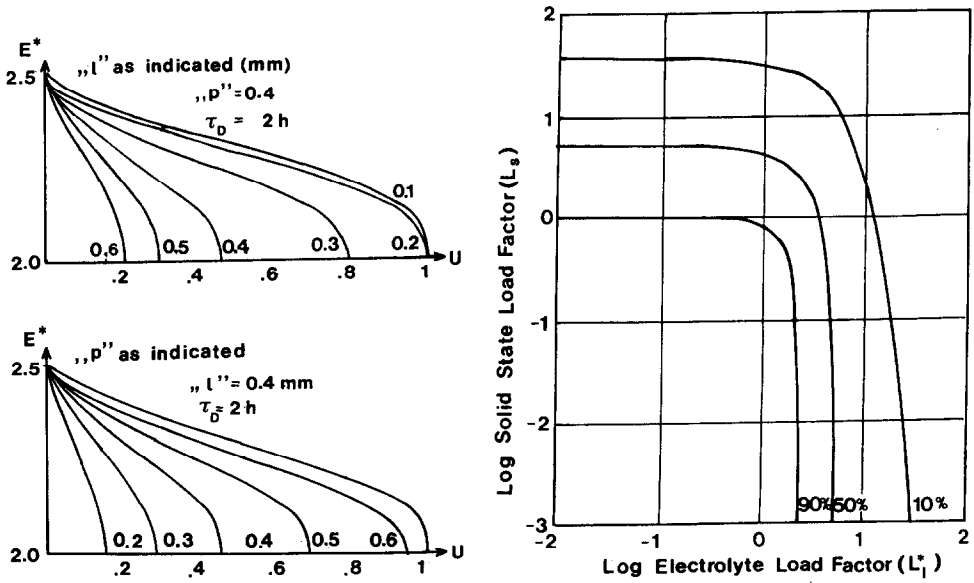

Fig. 6. Simulated discharge curves for a TiS_2 electrode with (a) different electrode thickness, $p = 0.4$, and (b) different porosities, $l = 0.4$ mm. $\tau_D = 2$ h, all other data as in Table 1.

Fig. 7. Load diagram for porous electrode with liquid electrolyte. "Iso utilization" contours for 90, 50 and 10% maximum utilizations. $L_s = \tau_s/\tau_D$. $L_l^* = \tau_l(1-p)c_s^o/\tau_D p c_l^o$. Geometry factor $s = 2$. Anion transport number 0.8.

Performing a number of simulations with L_s and L_l^* as variables the utilization was found and depicted as "iso utilization" contours in Fig. 7. It is obvious from the contours that, for small values of one load factor, the other controls the discharge. There is a transition region where solid state as well as electrolyte diffusion limits the discharge. In this region also, the electrode thickness and the particle size are as large as allowed by the discharge load and the requirement for a high utilization.

It is inherent in the mechanism causing electrolyte depletion that the anions leave the electrode pores. The mobility of the anions determines how fast this happens. The significance of this effect was investigated by performing simulations with the cation diffusion coefficient held at a fixed level, and with diminishing values of the anion diffusion coefficient. The results for a typical electrolyte-controlled electrode are shown in Fig. 8.

D_l as well as Λ decrease with D_-; however, a striking increase in coulombic capacity is obtained for very small values of D_-. The explanation is that the time constant for the electrolyte network increases so much that the insertion compound is exhausted before the near stationary state has occurred.

The composite insertion electrode

The term composite has been coined for an electrode consisting of insertion compound particles mixed with solid electrolyte particles [14].

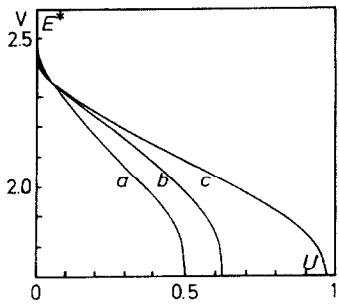

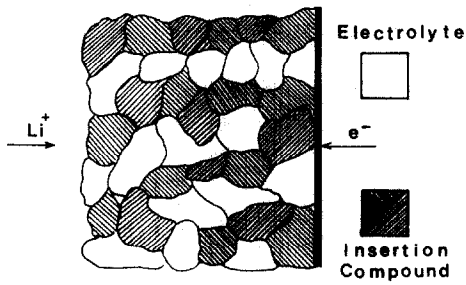

Fig. 8. Simulated discharge curves for varying anion diffusion coefficient. Electrode thickness, $l = 1$ mm; $\tau_D = 10$ h; $D_+ = 1.6 \times 10^{-6}$ cm^2 s^{-1}. (a) $D_- = 6.45 \times 10^{-6}$ cm^2 s^{-1} ($n_- = 0.8$); (b) $D_- = 1.8 \times 10^{-7}$ cm^2 s^{-1} ($n_- = 0.1$); (c) $D_- = 1.6 \times 10^{-8}$ cm^2 s^{-1} ($n_- = 0.01$). All other data as in Table 1.

Fig. 9. Two dimensional composite electrode concept.

The concept is illustrated in Fig. 9. The point is that true, solid ion conductors — excluding polymeric ion conductors — only show conductivity for one ionic species. When this is the inserted cation, the solid conductor can serve as electrolyte in the insertion electrode. As the "anions" — the compensating charges — are not mobile, electrolyte depletion cannot occur.

In this case, since dc/dz, dc/dt and D_1 are zero, most of the relations used in the preceding sections are not applicable. What remains are the basic relations:

$$i_t = -\frac{di'}{dz} \tag{1}$$

and in case the conductivity in the insertion compound network is large ($d\pi = 0$)

$$d\phi = -dE \tag{28}$$

and for the working potential

$$E^* = E_{surface} - E_{ref} \tag{29}$$

The transport relations for the electrolyte are reduced to:

$$i' = -\kappa_1 \frac{d\phi}{dz} \tag{32}$$

Using the macrohomogeneous model [8] κ_1 is the effective ionic conductivity of the composite structure. Combining these relations we get

$$i_t = -\kappa_1 \frac{d^2E}{dz^2} \tag{33}$$

i_t is the boundary condition for calculating the transport into the insertion compound using eqns. (7) and (8). Using the potential relation, eqn. (15), with c_1^* included in E°, the system can be solved numerically.

It is, however, possible to make some reasonable linearizations which allow an analytical solution. We assume that the insertion compound particles are so small that L_s is very small. Then the concentration on the surface of the particles will deviate negligibly from the average concentration. In this case we have $\partial X/\partial t = i_t/(F(1-p)c_s^\circ)$. Considering Fig. 3 it is obvious that the E/X relation can be linearized over a considerable range. Therefore we substitute eqn. (15) with a linear relation:

$$E = E^{\#} - kX \tag{34}$$

Using these approximations we get a second order partial differential relation for X.

$$\frac{\partial X}{\mathrm{d}t} = \frac{k\kappa_1}{F(1-p)c_s^\circ}\frac{\partial^2 X}{\mathrm{d}z^2} \tag{35}$$

As $\mathrm{d}X = -\mathrm{d}E/k = \mathrm{d}\phi/k$ we get the boundary conditions from eqn. (32)

$$\begin{aligned} &z = 0 \text{ (electrode surface)} \frac{\mathrm{d}X}{\mathrm{d}z} = -\frac{i^\circ}{k\kappa_1} \\ &z = l \text{ (current collector)} \frac{\mathrm{d}X}{\mathrm{d}z} = 0 \end{aligned} \tag{36}$$

Equations (35) and (36) have the same form as Fick's 2′ law for unidirectional diffusion in a bounded domain with constant flux into one boundary. The same relations control the diffusion in insertion compound particles. The "composite diffusion coefficient", D_c, is $k\kappa_1/F(1-p)c_s^\circ$. In other words, subject to the assumptions made in the derivation of eqn. (35), the composite electrode behaves as a solid slab of the insertion compound, but with the stoichiometric capacity reduced by a factor $1-p$. The transport properties are, however, considerably enhanced. Using Li_3N as electrolyte and $k = 26RT/F$ volt, the composite diffusion coefficient can be estimated as *ca.* 10^{-7} $cm^2\ s^{-1}$ compared with 10^{-10} - 10^{-12} $cm^2\ s^{-1}$ for most insertion compounds.

The solutions of eqns. (35) and (36) follow the same lines as discussed for the pure insertion compound, but only the solutions for $s = 1$ (plane geometry) are relevant. The time constant valid for the solution to eqn. (35) is

$$\tau_c = \frac{Fl^2(1-p)c_s^\circ}{k\kappa_1} \tag{37}$$

and the corresponding load factor

$$L_c = \frac{Fl^2(1-p)c_s^\circ}{\tau_D k\kappa_1} = \frac{Il^2}{k\kappa_1} \tag{38}$$

where the last form uses the discharge current per unit volume electrode. The working potential is $E^{\#} - kX^*$, where X^* is the value of X at the electrode surface. Two approximate solutions can be found for $t < \tau_c/3$ and

$t > \tau_c/3$ [14]. The discharge curve consists of two parts. A square root t (or U) part for $t < \tau_c/3$ (or $U < L_c/3$):

$$E^* = E^{\#} - 2k\left(\frac{L_c U}{\pi}\right)^{1/2} \tag{39}$$

and a linear part for $t > \tau_c/3$: $(U > L_c/3)$

$$E^* = E^{\#} - kU - k\frac{L_c}{3} \tag{40}$$

In the linear part, eqn. (40), the discharge potential should follow the e.m.f. curve only reduced by $kL_c/3$. Using the specific discharge current I, the depression is $I^2/3\kappa_1$. The utilization, estimated as the coulombic capacity until the working voltage decreases suddenly, cannot be estimated from the model described above, because the linear potential approximation used is invalid for $X \simeq 1$. However, the value of $U = U_{max}$ for $X^* = 1$ may be used as a rough estimate. In relation to the respective load factors this is the same as for the pure insertion compound with $s = 1$, eqn. (13).

A more detailed description requires that the nonlinear E/X relation, eqn. (15), is used, and that the condition of a small value of L_s is relaxed. The electrode is then treated by numerical simulation using the methods discussed for the porous electrode.

The most interesting case is still the performance if L_s is small. Simulated discharge curves for different values of L_c are shown in Fig. 10 [15]. For $U > L_c/3$, indicated by arrows on curves 1 - 3, it can be seen that the curves

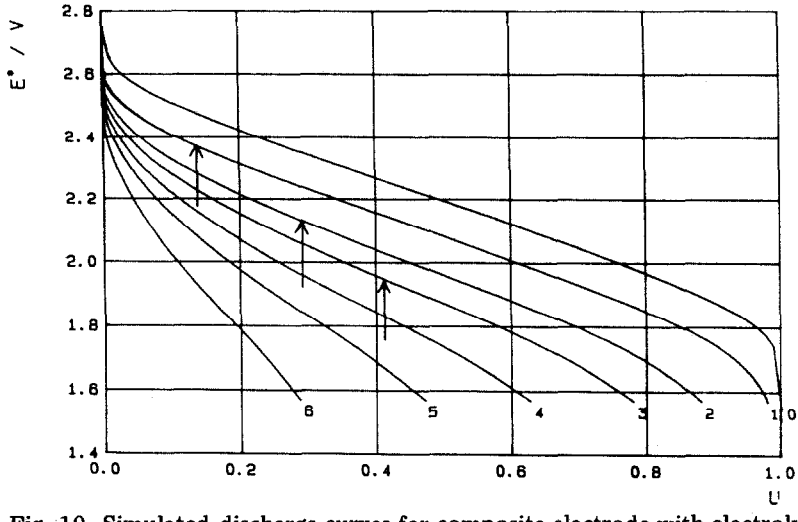

Fig. 10. Simulated discharge curves for composite electrode with electrolyte control. L_s = 0.025. 0: e.m.f; 1: L_c = 0.4; 2: L_c = 0.87; 3: L_c = 1.21; 4: L_c = 1.73; 5: L_c = 2.43; 6: L_c = 4.04. Arrows at 1, 2 and 3 indicate limit for the linear region.

run parallel with the e.m.f. curve, as predicted from eqn. (40), but they do not exhibit the sudden voltage decrease caused by the $\ln X/(1-X)$ term, eqn. (15), which expectedly should occur for potentials below 1.8 V. This is even more pronounced for curves 4 - 6 where the square root law, eqn. (39), applies.

The reason is that the electrode can be discharged further even if the insertion compound is saturated in the outer parts of the electrode. The inserted ions are still conducted into the interior of the electrode through the electrolyte, bypassing the saturated part. This mode of discharge continues until the local transfer current density in the still active part of the electrode increases so much, that the transport in the insertion compound particles becomes limiting. The working potential will be low because of the voltage loss in the electrolyte network. An approximate calculation for this part of the discharge predicts a dependence of $(1-U)^{1/2}$ [14]. The practical importance of this part of the discharge is, however, disputable because it occurs at such a low potential.

Conclusion

The use of insertion compounds as battery electrodes is limited by the requirement that the inserted ion must be distributed in the interior of the insertion compound particle. The transport necessary for this is solid state diffusion, which is slow compared with the required discharge rates. In the porous and composite electrodes the electrolyte takes care of the ionic transport into the electrode. In practical batteries, the transport in the electrolyte often becomes limiting for the rate capability because of the desire to use as thick an electrode as possible. Due to the mobility of the anions in liquid electrolytes this limitation may manifest itself as electrolyte depletion in the interior of the electrode. This prevents utilization of the active mass there.

The limitation is overcome by using a true solid, (not polymeric) electrolyte in the so-called composite electrode. The low room-temperature conductivity and poor technological properties of known solid electrolytes makes the general use of this possibility difficult.

The load factors are used to estimate which transport processes limit the utilization of the active material. The magnitude of the electrolyte load factor indicates whether, or not, electrolyte depletion will occur. If the insertion compound or the composite load factor is dominating, they allow estimates of the maximum utilization.

List of symbols

A^+	Inserted alkali metal ion
b	Mobility in insertion compound

c_1	Concentration of electrolyte salt in electrolyte
c_1^*	c_1 at interface
c_1^o	c_1 at electrode surface
c'	Concentration of electrolyte salt per unit volume electrode
c_s	Concentration of A in insertion compound
c_s^o	Saturation value of c_s
D_s	Solid state diffusion coefficient
D_+, D_-	Ionic diffusion coefficients in electrolyte
D_1	Electrolyte salt diffusion coefficient
D_1'	Effective salt diffusion coefficient in electrode
D_c	Apparent diffusion coefficient in composite electrode
E	Electrode potential against a reversible Li electrode
E^o	Standard electrode potential
E^*	Discharge potential of porous and composite electrode
$E^\#$	Constant in linearization of eqn. (15)
F	Faraday constant
f	Interaction parameter in eqn. (5)
HA_x	Insertion compound
I	Discharge current per unit volume electrode
I_y	Dimensionless transfer current [12]
i_1	Ionic current density in electrolyte pores
i'	Ionic current density in composite electrode
i_t	Transfer current
i_y	Transfer current density
i^o	Discharge current density at electrode surface
j	Flux density
j_+, j_-	Flux density for cations and anions in electrolyte pores
$K_{+,o}; K_{-,o}$	Friction coefficients between ions and solvent
$K_{+,-}$	Mutual friction coefficient between cation and anion
k	Constant in linearization of eqn. (15)
L_s	Load factor for insertion compound particle
L_1	Load factor for electrolyte pores
L_1^*	Modified electrolyte load factor
L_c	Load factor for composite electrode
l	Thickness of porous and composite electrode (from surface to current collector)
n_+, n_-	Transport numbers
p	Volume fraction of electrolyte (porosity)
Q_o	Charge per unit volume electrode
RT	Product of gas constant and absolute temperature
r	Distance from center to surface of insertion compound particle
s	Geometry factor
t	Time
U	Degree of discharge (t/τ_D)
v_+, v_-	Ionic velocities
X	Degree of insertion (c_s/c_s^o)

y	Spatial coordinate in insertion compound
z	Spatial coordinate in porous or composite electrode

Greek letters

δ	Small increment
ϕ	Galvani potential in electrolyte
$\mu^{\ominus}$	Standard chemical potential
μ_s	Chemical potential of inserted ion
μ_e	Chemical potential of electrons
μ_+, μ_-	Chemical potential of cation and anion in electrolyte
$\bar{\mu}_i$	Electrochemical potentials $\bar{\mu}_i = \mu_i \pm F\phi$
κ_l	Ionic conductivity
Λ	Molar conductance
π	Fermi potential in insertion compound
θ	Tortuosity
τ_c	Time constant for composite electrode
τ_D	Stoichiometric discharge time (Q_o/I)
τ_l	Time constant for diffusion in electrolyte pores
τ_s	Time constant for diffusion in insertion compound particle

References

1 M. Armand, *Diss. Inst. Nat. Polytechn. Grenoble*, Feb. 7, 1979.
2 W. R. McKinnon and R. R. Haering, in *Modern Aspects of Electrochemistry, 15* (1979) 235.
3 S. Atlung, K. West and T. Jacobsen, *J. Electrochem. Soc., 126* (1979) 1311.
4 S. Atlung and T. Jacobsen, *Electrochim. Acta, 26* (1981) 1477.
5 K. West, T. Jacobsen and S. Atlung, Dynamics of porous solid solution electrodes, *Paper 174, The Electrochemical Society 156th Meeting, Los Angeles, Oct. 14 - 19, 1979.*
6 K. West, T. Jacobsen, B. Zachau-Christiansen and S. Atlung, *Ext. Abstracts, A11, 32nd ISE Meeting, Dubrovnik, 1981.*
7 J. Newman, D. Bennion and C. W. Tobias, *Ber. Bunsenges. Phys. Chem., 69* (1965) 608; K. Micka, *72* (1968) 60.
8 J. Newman and C. W. Tobias, *J. Electrochem. Soc., 109* (1962) 1183.
9 S. Atlung, *J. Power Sources, 13* (1984) 54.
10 H. S. Carslaw and J. C. Jaeger, *Conduction of Heat in Solids*, Oxford University Press, 2nd edn., 1959, pp. 130.
11 T. R. Brumleve and R. P. Buck, *J. Electroanal. Chem., 49* (1978) 1.
12 K. West, T. Jacobsen and S. Atlung, *J. Electrochem. Soc., 129* (1982) 1480.
13 S. Atlung, K. West and T. Jacobsen, in D. W. Murphy, J. Broadhead and B. C. H. Steele (eds.), *Materials for Advanced Batteries*, Plenum Publishing Corp., New York, 1980, pp. 275.
14 S. Atlung, B. Zachau-Christiansen, K. West and T. Jacobsen, *J. Electrochem. Soc., 131* (1984) 1200.
15 Boye C. Knutz, *Thesis*, The Technical University, Lyngby, Denmark, 1985, to be published.